

UCRL-JC-132488

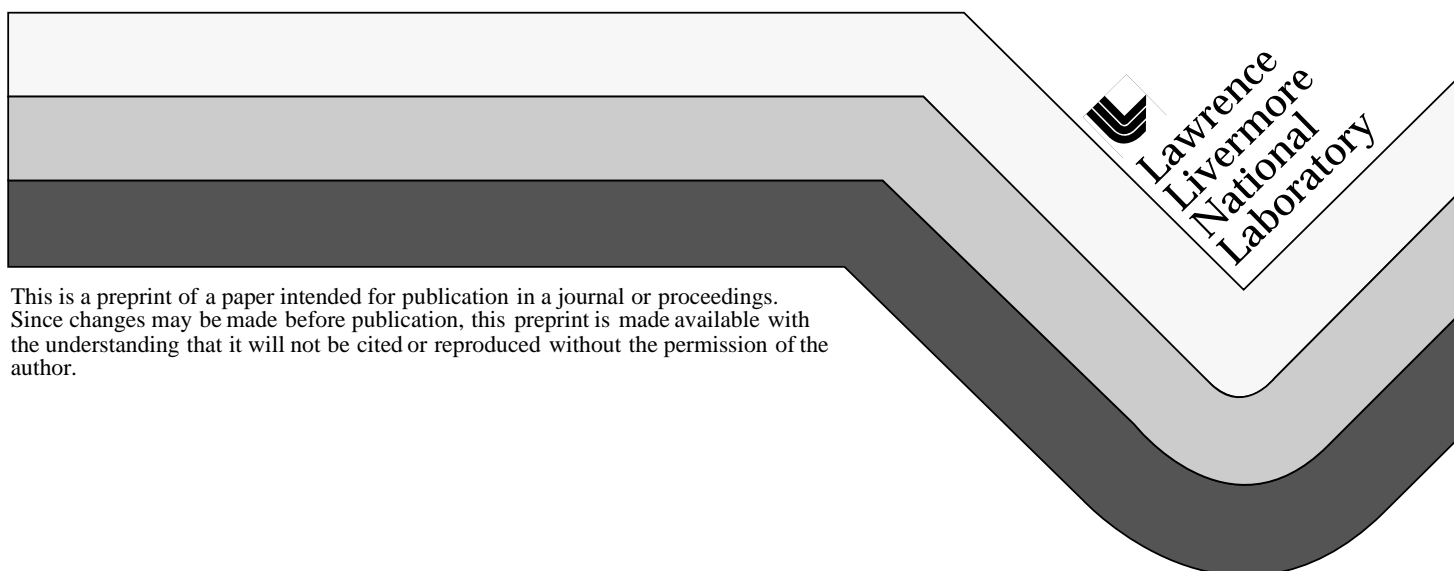
PREPRINT

# **A New Mechanical Characterization Method for Microactuators Applied to Shape Memory Films**

Kirk P. Seward  
Peter Krulevitch  
Harold D. Ackler  
Philip B. Ramsey

This paper was prepared for submittal to the  
Transducers '99  
The 10th International Conference on Solid-State Sensors and Actuators  
Senda, Japan  
June 7-10, 1999

**March 1999**



#### DISCLAIMER

This document was prepared as an account of work sponsored by an agency of the United States Government. Neither the United States Government nor the University of California nor any of their employees, makes any warranty, express or implied, or assumes any legal liability or responsibility for the accuracy, completeness, or usefulness of any information, apparatus, product, or process disclosed, or represents that its use would not infringe privately owned rights. Reference herein to any specific commercial product, process, or service by trade name, trademark, manufacturer, or otherwise, does not necessarily constitute or imply its endorsement, recommendation, or favoring by the United States Government or the University of California. The views and opinions of authors expressed herein do not necessarily state or reflect those of the United States Government or the University of California, and shall not be used for advertising or product endorsement purposes.

# A NEW MECHANICAL CHARACTERIZATION METHOD FOR MICROACTUATORS APPLIED TO SHAPE MEMORY FILMS

Kirk P. Seward\*, Peter Krulevitch, Harold D. Ackler, and Philip B. Ramsey

Lawrence Livermore National Laboratory Center for Microtechnology

\*and Massachusetts Institute of Technology

7000 East Ave., L-222, Livermore, CA 94550

phone: (925) 422-9195 fax: (925) 422-2373 email: [seward2@llnl.gov](mailto:seward2@llnl.gov)

## ABSTRACT

We present a new technique for the mechanical characterization of microactuators and apply it to shape memory alloy (SMA) thin films. A test instrument was designed which utilizes a spring-loaded transducer to measure displacements with resolution of 1.5  $\mu\text{m}$  and forces with resolution of 0.2 mN. Employing an out-of-plane loading method for SMA thin films, strain resolution of 30  $\mu\epsilon$  and stress resolution of 2.5 MPa were achieved. Four mm long, 2  $\mu\text{m}$  thick NiTiCu ligaments suspended across open windows were bulk micromachined for use in the out-of-plane stress and strain measurements. Static analysis showed that 63% of the applied strain was recovered while ligaments were subjected to tensile stresses of 870 MPa. This corresponds to 280  $\mu\text{m}$  of actual displacement against a load of 52 mN. Fatigue analysis of the ligaments showed 33% degradation in recoverable strain (from 0.3% to 0.2%) with  $2 \times 10^4$  cycles for an initial strain of 2.8%.

## INTRODUCTION

Micro-Electromechanical Systems (MEMS) often rely on thin film actuators and structural members. The design of systems employing these films necessitates an understanding of their mechanical characteristics. Because film properties vary with distinct fabrication methods, and even from run to run, a simple technique to provide all necessary mechanical data is beneficial.

Thin film shape memory alloys in particular require characterization for device qualification because the material's behavior is sensitive to processing conditions and alloy composition. A number of researchers have concentrated their efforts on developing models of these alloys, but it is difficult to predict their behavior based solely on processing knowledge. The instrument described in this paper can be used to test SMA film microactuators in a non-destructive manner. It provides a comprehensive range of thermomechanical information with simultaneous determination of stress-strain behavior and material resistivity of both phases, recoverable stress against a load, fatigue behavior, response and cycling times, actuator displacement, and power requirements. Previous experimental methods and their measurement capabilities are compared in Table 1.

This testing instrument also has utility in measuring the response of other microactuators. For example, applying a point load at the end of a piezoelectric cantilever with the transducer discussed in this paper allows for the simultaneous measurement of force and displacement, yielding the bending moment. Displacement and actuation force can then be determined as a function of applied voltage.

Table 1: Comparison of existing SMA characterization methods with new out-of-plane ligament test.

Testing method	Transf. Temp.	Resistivity	Stress-strain	In-line testing	Non-destructive
Tensile test [1]		*	✓		
Film resistivity [2]	✓	✓		*	✓
Wafer curvature [3]	✓		†	‡	✓
Scanning calorimetry [1,2]	✓				
Diaphragm bulge tests [4]			✓	*	✓
Out-of-plane ligament test		✓	✓	✓	✓

\* Possible

† Yes, but not flexible

‡ Not on actual parts

## TESTING METHOD

Unlike more traditional mini-tensile testing schemes, in which strips of SMA film are totally or partially freed from the substrate and pulled upon [1], the tests described in this paper utilize out-of-plane stretching without detachment from the substrate. Freestanding NiTiCu ligaments test chips (see Fig. 1) were created using Si micromachining. One cm square unpatterned (blank) chips were processed on the same substrate as the ligament structures for use in curvature measurements.

Because film thickness was much less than ligament width, out-of-plane loading produced negligible bending stresses, and the ligaments were assumed to be in a state of uniaxial tension. A spring-loaded differential variable reluctance transducer (DVRT) [5] was used to measure ligament deflection with uncertainty of  $\pm 1.5 \mu\text{m}$ , and reaction forces were calculated based on the calibration of the spring constant ( $0.186 \pm 0.002 \text{ N/mm}$ ). The corresponding force, stress, and strain resolutions were 0.2 mN, 2.5 MPa, and 30  $\mu\epsilon$ , respectively.

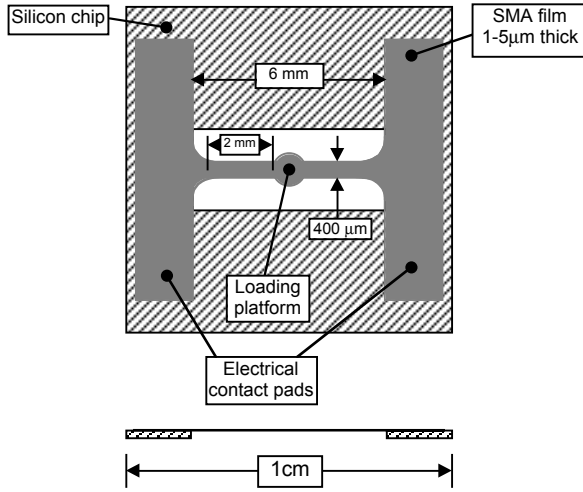


Figure 1: NiTiCu test chips consist of freestanding ligaments over an open window in a 1 cm square Si chip.

Measurements were initiated by positioning the conical DVRT head using a precision micrometer head with resolution of  $\pm 1 \mu\text{m}$  [6] and XY-translation stage until contact was established with the test ligament, as seen in Fig. 2a. At this point, the micrometer head and DVRT output were set to zero. This step in the process added the most uncertainty to the measurement because contact was measured visually through a magnifying lens.

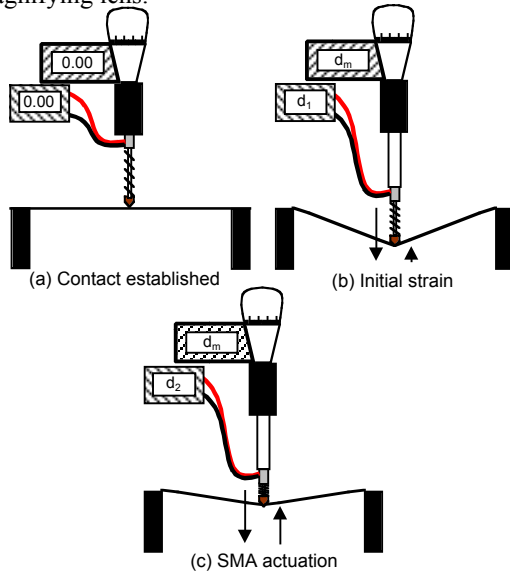


Figure 2: The DVRT head measures displacements and forces of the ligament as the digital micrometer is advanced. The micrometer displacement and the DVRT compression are displayed on digital readouts during each step of the measurement. SMA actuation is caused by resistive heating of the ligament.

To measure static stress-strain behavior for a film, the micrometer is advanced, compressing the spring and deforming the film. The total displacement of the center of the ligament is the difference between the micrometer reading  $d_m$  and DVRT reading  $d_l$  as seen in Fig. 2b. The downward force on the ligament is equal to the product of the spring compression and spring

constant ( $d_l \times k$ ). The tension and axial displacement of the film are determined by a simple geometric calculation. By resistively heating the ligament, the DVRT spring compresses to a value  $d_2 > d_1$  (see Fig. 2c), resulting in greater ligament stress while reducing the ligament strain. The stress created in the film during this process is known as the recoverable stress  $\sigma_{rec}$ . The difference between the initial strain and final strain is the recoverable strain  $\epsilon_{rec}$ , which is divided by the initial strain on the ligament to give the percentage of strain recovered by actuation  $\epsilon\%$ .

Shape memory actuation occurs when the ligament is heated and the solid-solid phase transformation occurs between the highly twinned, ductile, room temperature martensite phase to the high temperature austenite phase. This phase transformation causes the recovery of twins and allows the material to “remember” its original shape [7,8].

Using the measured deflections, ligament geometry, and Eqs. 1 and 2, the recoverable stress  $\sigma_{rec}$  and percentage of strain recovered  $\epsilon\%$  were found. Equation 1 was used to calculate the initial stress (Fig. 2b) and the final stress (Fig. 2c). Equation 2 finds its basis in the definition of true strain. In this equation, the value  $L_0$  is the original unstrained gauge length of one leg of the ligament. This unstrained length takes into account the residual strain in the ligament, and can be measured by either of two methods. The first involves fracturing a ligament, heating it, and measuring the unstrained length. This length can also be measured non-destructively, however, by back-calculation from curvature measurements of the residual stress.

$$\sigma_{1,2} = \frac{k d_{1,2}}{w h \sin \theta_{1,2}} \quad (1)$$

$$\epsilon_{1,2} = \ln\left(\frac{L'}{L_0}\right) = \ln\left(\frac{L}{\cos \theta_{1,2} L_0}\right) \quad (2)$$

$k$  = DVRT spring constant = 0.186 N/mm

$w$  = ligament width

$h$  = ligament thickness

$d_{1,2}$  = initial, final DVRT compression

$\theta_{1,2}$  = initial, final angle between ligament and horizontal

$L_0$  = initial unstrained ligament gauge length

$L'$  = final stretched length of ligament gauge section for one leg

$L$  = gauge section length of one ligament leg

## EXPERIMENTAL PROCEDURES

Four inch diameter, 380  $\mu\text{m}$  thick {100} Si wafers coated with 0.6  $\mu\text{m}$  wet, thermally grown  $\text{SiO}_2$  served as substrates for the SMA films. Nickel-titanium-copper films were DC magnetron sputter-deposited at 150 W from a 33 mm diameter NiTiCu target while heating the substrate. Films were deposited in a high vacuum chamber under  $5.4 \times 10^{-8}$  to  $1.9 \times 10^{-7}$  Torr base pressure in 8 mTorr argon. Thermocouples

mounted to the Si substrate surface indicated substrate temperatures of 510 °C at deposition start and 540 °C upon termination. A deposition time of 2 hours resulted in average film thickness across the wafer of 1.9  $\mu\text{m}$  with variations of  $\pm 0.4 \mu\text{m}$ . Thickness variation was due to the low target to substrate diameter ratio, resulting in the thickest film depositing directly in line with the target and diminished film thickness from the center to the edge of the wafer. Film composition, measured by electron microprobe analysis, was 39.5at%Ni, 52at%Ti, and 8.5at%Cu.

The test chips were distributed across the wafer with the ratio of four ligament test chips for every blank substrate curvature test chip. The ligaments were patterned by wet chemical etching of the NiTiCu using 20HCl:20HNO<sub>3</sub>:1HF. The SiO<sub>2</sub> coating on the wafer prevented Si etching during this step. Windows were etched from the backside of the wafers using an STS deep reactive ion etching system with a plasma chemistry of C<sub>4</sub>F<sub>8</sub> for passivation and SF<sub>6</sub> for Si etching. Subsequent reactive ion etching in a 10:1 CF<sub>4</sub>:O<sub>2</sub> plasma removed all remaining SiO<sub>2</sub>, freeing the ligaments.

Ligament actuation measurements involved deflecting a ligament, taking a martensite measurement of stress and strain, and then heating the ligament and taking an austenite measurement. Currents of  $\sim 0.15 \text{ A}$  and voltages of  $\sim 1.9 \text{ V}$  (power  $\approx 0.29 \text{ W}$ ) were ascertained by increasing the power through the ligament until maximum actuation was encountered. These measurements were performed over a range of initial strains. A series of stress-strain measurements were also taken at room temperature and another series at constant applied power. Cycling ligaments with a voltage square wave and digitally acquiring the DVRT output produced fatigue measurements. Voltage and cycling times were tuned to realize maximum cycling frequency while ensuring full phase transformation.

Curvature tests were performed to quickly confirm shape memory behavior, measure residual stresses, and find transition temperatures of the film. Curvature of the blank chips was measured as a function of temperature using a Tencor FLX-2320 film stress measurement system, ramping at 3 °C/min between room temperature and 100 °C. The average biaxial residual stress was calculated by the well known modified Stoney equation [9] with a biaxial modulus  $E_s/(1-\nu_s)$  equal to 180.5 GPa for {100} silicon [10], substrate thickness  $t_s$  of 380  $\mu\text{m}$  and film thickness  $t_f$  measured by a stylus tip profilometer.

## RESULTS AND DISCUSSION

Curvature results for seven chips from the same substrate are shown in Fig. 3. The residual stress in the martensite phase, equivalent to the martensitic yield stress [3], was 108 MPa averaged over all test chips.

Transition temperatures were  $A_s=50^\circ\text{C}$ ,  $A_f=61^\circ\text{C}$ ,  $M_s=58^\circ\text{C}$  and  $M_f=37^\circ\text{C}$  ( $A$ =austenite,  $M$ =martensite,  $s$ =start,  $f$ =finish), and the recoverable stress, seen in Fig. 3, was 500 MPa.

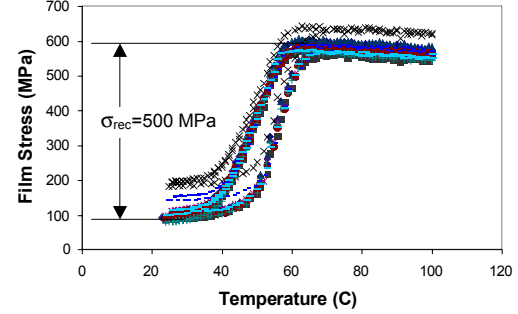


Figure 3: Curvature measurements of 7 different test chips illustrate uniformity of shape memory effect across a wafer.

The results for one ligament are illustrated in Figs. 4 and 5, with measurement error included. For this particular ligament, maximum actuation of 300  $\mu\text{m}$  and actuation forces of 56 mN were found for an initial ligament deflection of 750  $\mu\text{m}$ . Work output from the ligament (the product of actuation force and displacement) rose to 60  $\mu\text{J}$  before fracture of the ligament at 8.5% initial true strain. Figures 4 and 5 depict a maximum recoverable stress of 700 MPa at 4.4% initial true strain and maximum percentage of true strain recovery of 63% at 3.4% initial true strain while under 870 MPa of initial stress. This data point corresponded to 280  $\mu\text{m}$  of actuation under a 52 mN initial force.

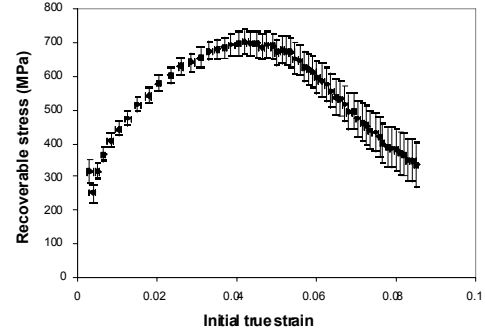


Figure 4: Recoverable uniaxial stress of a ligament versus the initial true strain found by out-of-plane deflection and subsequent actuation.

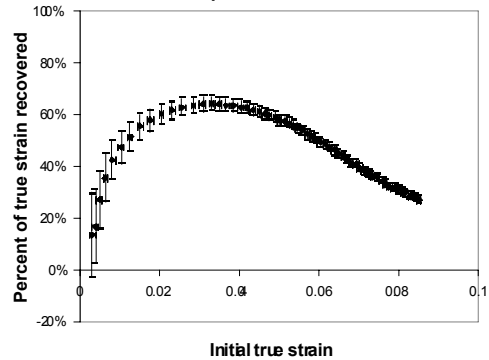


Figure 5: The percentage of true strain recovered versus the initial true strain gives an indication of the volume fraction of twin recovery with initial strain.

An interesting phenomenon seen in Figs. 4 and 5 is the fact that both curves reach a maximum value at some initial true strain. Part of this can be accounted for by the martensite stress increasing after all twin motion has occurred, thus lowering the difference between martensite and austenite stress. However, we also presume that a stress induced martensite effect is happening. The applied power was based upon minimum requirements at low stress and not increased with loading. Thus, at high stress, less strain was recovered due to the Clausius-Clapeyron relationship, which shifts full transformation to higher temperatures.

The martensite yield stress (biaxial residual stress) was found by taking initial curvature measurements at room temperature for the blank chips. To calculate the uniaxial residual stress in the ligaments, the measured biaxial stress of 108 MPa was multiplied by  $(1-\nu)$ . Using a Poisson's ratio  $\nu$  of 0.33 for bulk NiTiCu, the resulting residual uniaxial stress  $\sigma_0$  was 72 MPa. The residual stress and strain are included in the curves plotted in Fig. 6, which show data from five ligaments loaded to fracture at room temperature and five at elevated temperature. No permanent, irrecoverable plastic deformation was observed when ligaments were loaded, unloaded and heated to austenite before the occurrence of fracture.

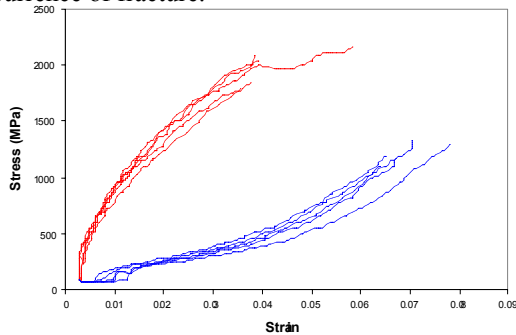


Figure 6: Stress-strain curves corrected for residual stress and strain for five low temperature (lower slope) and five high temperature (higher slope) ligaments.

Fatigue data from three ligaments is seen in Fig. 7. These tests were performed at 5 Hz with full transformation occurring for each ligament for the entire test, terminating at fracture for each ligament. Degradation in recovered strain of roughly 25% was noticed at  $2 \times 10^5$  cycles and 2.2% initial strain.

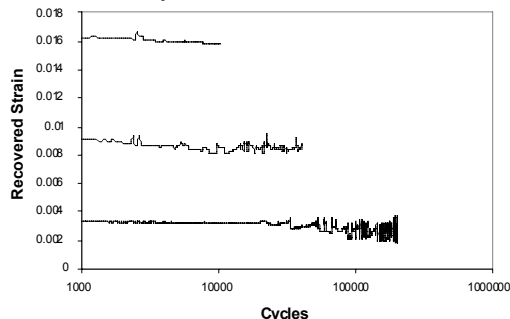


Figure 7: Cycles to failure for 3 different ligaments run at 5 Hz. Recovered strain diminished slightly for each of the ligaments.

Resistance measurements were taken concurrently with fatigue cycling. The resistance decrease upon entering the austenite phase was seen, as predicted, from 25  $\Omega$  martensite resistance to 22  $\Omega$  austenite resistance.

## SUMMARY

Performing a comprehensive engineering analysis of NiTiCu facilitates the design of MEMS devices that employ SMA films. The tests performed with the out-of-plane ligament deflection instrument proved that quantitative, simultaneous measurements of stress and strain can be made on thin film SMAs. Not limited to SMA films, this testing method can be applied to other films and microactuators with characteristic dimensions upwards of 100  $\mu\text{m}$  to find stress-strain characteristics for thin film materials, ultimate tensile strength of brittle films, and force versus displacement data for actuators.

For the materials scientist, the percentage of true strain recovered in Fig. 5 indicates that the volume fraction of twin recovery decreases with increased loads due to stress induced martensite. For the design engineer, recoverable stress data from ligament tests can now be calibrated with curvature data to determine design constraints, allowing the creation of freestanding structures with predictable behavior. And for the manufacturing engineer, this instrument is simple enough to use for non-destructive in-line testing and quality control in fabrication processes.

## ACKNOWLEDGEMENTS

Special thanks to Mike McGregor for melting the NiTiCu ingot used for making targets and to Julie Hamilton and Dino Ciarlo for guidance in the microfabrication of the test chips. This work was performed under the auspices of the US Department of Energy by the Lawrence Livermore National Laboratory under contract W-7405-ENG-48.

## REFERENCES

1. S. Miyazaki, K. Nomura, A. Ishida and S. Kajiwar, "Recent Developments in Sputter-Deposited Ti-Ni-Base Shape Memory Alloy Thin Films," *Journal de Physique IV France*, vol. 7, Col. C5, pp. 275-280, 1997.
2. A. D. Johnson, "Vacuum-deposited TiNi shape memory film: characterization and applications in microdevices," *J. Micromech. Microeng.*, vol. 1, pp. 34-41, 1991.
3. P. Krutvitch, A. P. Lee, P. B. Ramsey, J. C. Trevino, J. Hamilton and M. A. Northrup, "Thin Film Shape Memory Alloy Microactuators," *J. Microelectromechanical Systems*, vol. 5, no. 4, pp. 270-282, December 1996.
4. R. H. Wolf and A. H. Heuer, "TiNi (Shape Memory) Films for MEMS Applications," *J. Microelectromechanical Systems*, vol. 4, pp. 206-212, December 1995.
5. Microminiature DVRT, Microstrain, Inc., 294 N. Winooski Ave., Burlington, VT, USA 05401.
6. Digimatic Micrometer Head, Part #350-712-30, Mitutoyo/MTI, 16925 Gale Ave., City of Industry, CA, USA 91745.
7. H. C. Ling and R. Kaplow, "Phase Transitions and Shape Memory in NiTi," *Metallurgical Transactions A*, vol. 11A, pp. 77-83, January 1980.
8. K. Bhattacharya, in *Shape Memory Alloys: From Microstructure to Macroscopic Properties*, G. Airoldi, I. Müller and S. Miyazaki, Eds., Trans Tech Publications, 1997.
9. R. W. Hoffman, in *Physics of Thin Films*, vol. 3, G. Hass and T. E. Thun, Eds., New York: Academic, 1996.
10. W. A. Brantley, *Journal of Applied Physics*, vol. 44, p. 543, 1973.